Published in final edited form as:
Chem Res Toxicol. 2013 June 17; 26(6): 976–985. doi:10.1021/tx4001286.

Cysteine-conjugated metabolite of ginger component [6]-shogaol serves as a carrier of [6]-shogaol in cancer cells and in mice

Huadong Chen[†], **Dominique N. Soroka**[†], **Yingdong Zhu**[†], **Yuhui Hu**[‡], **Xiaoxin Chen**[‡], and **Shengmin Sang**[†,*]

[†]Center for Excellence in Post-Harvest Technologies, North Carolina Agricultural and Technical State University, North Carolina Research Campus, 500 Laureate Way, Kannapolis, NC 28081, USA

[‡]Cancer Research Program, Julius L. Chambers Biomedical/Biotechnology Research Institute, North Carolina Central University, 700 George Street, Durham, NC 27707, USA

Abstract

Shogaols, a series of major constituents in dried ginger (*Zingiber officinale*), show high anti-cancer potencies. Previously, we reported that a major metabolite resulting from the mercapturic acid pathway, 5-cysteinyl-[6]-shogaol (M2), showed comparable growth inhibitory effects towards cancer cells to [6]-shogaol (6S). Here we probe the mechanism by which M2 exerts its bioactivity. We utilized a series of chemical stability tests in conjunction with bioassays to show that thiol-conjugates display chemopreventative potency by acting as carriers of active ginger component 6S. M2 chemical degradation to 6S was observed in an environment most resembling physiological conditions, with a pH of 7.4 at 37°C. The metabolic profiles of M2 in cancer cells HCT-116 and H-1299 resembled those of 6S, indicating that its biotransformation route was initiated by deconjugation. Further, the presence of excess glutathione significantly delayed 6S and M2 metabolism and counteracted cell death induced by 6S and M2, suggesting that increasing available free thiols exogenously both promoted formation of 5-glutathionyl-[6]-shogaol (M13) and inhibited the production of free 6S from M2 deconjugation, resulting in delayed 6S cell entry and bioactivity. Given the chemopreventative properties of M2 and our observations *in vitro*, we investigated its metabolism in mice. M2 and 6S showed similar metabolic profiles in mouse urine and fecal samples. Six new thiol-conjugated metabolites (M16–M21), together with previously reported ones, were identified by LC/MS. In particular, the increase of 5-N-acetylcystenyl-[6]-shogaol (M5) and its 3′-demethylated product (M16) abundance in mouse feces after treatment with M2 indicate that in addition to acting as a carrier of 6S, M2 is also directly acetylated to M5, which is further demethylated to M16 in vivo. In conclusion, cysteine-conjugated metabolite of [6]-shogaol M2 exerts its bioactivity by acting as a carrier of 6S in both cancer cells and in mice.

Keywords

ginger; [6]-shogaol; 5-cysteinyl-[6]-shogaol; carrier; metabolism; cancer cells; mice

[*]**Corresponding Author:** Center for Excellence in Post-Harvest Technologies, North Carolina Agricultural and Technical State University, North Carolina Research Campus, 500 Laureate Way, Kannapolis, NC 28081. Tel: 704-250-5710. Fax: 704-250-5709. ssang@ncat.edu.

Supporting Information Available: Stability of M2, structure elucidation of M19–21, and chromatograms of M2 diastereoisomers are in Supporting Information file. This material is available free of charge via the Internet at http://pubs.acs.org.

Introduction

Ginger, the rhizome of *Zingiber officinale*, has been utilized for thousands of years as a spice and crude drug. It has been an integral part of traditional Eastern medicine since ancient times and is considered a tonic root for ailments including: stomach pain and nausea, cholera, asthma, heart conditions, respiratory disorders, toothaches, and rheumatic complaints[1–3]. The major pharmacologically active components of ginger are gingerols and shogaols[4], which have both been implicated in chemoprevention over the past decade[3, 5–10]. Shogaols are the products of gingerols after thermal processing and are the primary constituents of dried ginger[4]. Studies have shown that shogaols have greater anti-carcinogenic activity than their precursors. For example, in a study by Kim et al, [6]-shogaol (6S, Figure 1) exhibited greater growth inhibitory effects in A-549 human lung cancer cells, HCT-15 human colon cancer cells, SK-OV-3 human ovarian cancer cells, and SKMEL-2 human skin cancer cells than [4]-, [6]-, [8]-, and [10]- gingerols[11]. Bak *et al.* established that mice treated with ginger extract high in shogaols displayed an up-regulation of antioxidant response with drastically increased Nrf2 expression in derived liver samples[12]. Additionally, Hu et al. showed that 6S induced apoptosis, caspase activation, and Poly (ADP-ribose) polymerase (PARP) cleavage in both SMMC-7721 human hepatocellular carcinoma cells and SMMC-7721 tumor xenografts through an endoplasmic reticulum (ER) stress-associated mechanism[13]. Furthermore, our group demonstrated that [6]-, [8]-, and [10]-shogaols exhibited significantly higher toxicity to HCT-116 human colon and H-1299 human lung cancer cells than [6]-, [8]-, and [10]-gingerols[14]. With our collaborators, we have also found that 6S was more effective than [6]-gingerol in inhibiting 12-*O*-tetradecanoylphorbol 13-acetate (TPA)-induced tumor promotion in mice[15].

Recent studies from our group have established that 6S is extensively metabolized in mice and in cancer cells[16, 17]. By examining the biotransformation of 6S, we found that the mercapturic acid pathway and a redox pathway are its major metabolic routes[16, 17]. As previously reported, an initial reaction between the α,β-unsaturated ketone functional group of 6S and the cysteine sulfhydryl group of glutathione (GSH) takes place in the mercapturic acid pathway, giving rise to the corresponding conjugates. The conjugates then undergo successive enzymatic modifications on the GSH moiety, forming cysteinylglycine-, cysteine-, and finally N-acetylcysteine conjugates, which are excreted in the urine or feces. To test the bioactivity of the metabolites of 6S, our group synthesized these major metabolites and tested each for growth inhibition of HCT-116 human colon and H-1299 human lung cancer cells[18]. The compound that displayed the highest potency was the cysteine conjugate of 6S (M2, Figure 1), which showed comparable potency to parent 6S (IC_{50} values of 24.43 and 25.82 μM versus 18.20 and 17.90 μM in HCT-116 and H-1299 cells, respectively). The high efficacy of metabolite M2 against cancer cells was complimented by its comparatively low toxicity to human normal fibroblast colon cells CCD-18Co and human normal lung cells IMR-90 with IC_{50} values of 99.18 and 98.30 μM, respectively[18]. TUNEL assay also indicated apoptosis in cancer cells was triggered by thiol-conjugated metabolite M2[18].

Given the high potency of conjugate metabolite M2 versus the relatively weak activity of the remaining metabolites, it was necessary to further investigate this compound to elucidate its mechanism of action. Organic isothiocyanates (ITC's) also undergo metabolism via the mercapturic acid pathway to form thiol-conjugates. The biological relevance of the transformation products has been attributed to their activities as hydrophilic carriers of ITC's, which are relatively unstable and readily dissociate to their parent compounds, resulting in similar observed chemopreventative properties as the parents[19, 20]. Phase II metabolism products such as thiol-conjugates are more water soluble and often less toxic and pungent than their parent compounds, making them preferable for chemoprevention

trials[21]. Given this possible application for the thiol-conjugated metabolites of 6S, the following study is an investigation of the notion that metabolite M2 exerts its anti-cancer potency by acting as a carrier of its parent molecule.

Materials and methods

Materials

6S was purified from ginger extract in our laboratory[14]. M2 was synthesized in our laboratory, as previously reported[18]. HPLC-grade solvents and other reagents were obtained from VWR International (South Plainfield, NJ). LC/MS grade solvents and other reagents were obtained from Thermo Fisher Scientific (Pittsburgh, PA). Glutathione, sulfatase from *Aerobacter aerogenes*, and β-glucuronidase from *Helix aspersa* were obtained from Sigma (St. Louis, MN).

Treatment of mice and urine collection

Experiments with mice were carried out according to protocols approved by the Institutional Review Board for the Animal Care and Facilities Committee at North Carolina Central University. In brief, female C57BL/6J mice were purchased from the Jackson Laboratory (Bar Harbor, ME, USA) and allowed to acclimate for at least 1 week prior to the start of the experiment. The mice were housed 5 per cage and maintained in air-conditioned quarters with a room temperature of 20 ± 2 °C, relative humidity of 50 ± 10%, and an alternating 12-h light/dark cycle. Mice were fed Purina Rodent Chow #5001 (Research Diets) and water, and were allowed to eat and drink *ad libitum*. 6S or M2 in dimethyl sulfoxide (DMSO) were administered to mice by oral gavage (200 mg/kg). Urine and fecal samples were collected in metabolism cages (5 mice per cage) 24 h after administration of vehicle (control group, n = 5), 6S (treated group, n = 5), or M2 (treated group, n=5). The samples were stored at −80 °C until analysis.

Urine and fecal samples preparation

For acquisition of the metabolic profile, six pieces of each fecal sample (control and treated) were selected and placed in 2 mL tubes. Each set was weighed and 1.0 mL of MeOH with 0.2% acetic acid was added to each sample. Samples were homogenized 90 s by an Omni Bead Ruptor Homogenizer (Kennesaw, GA) and then centrifuged at 17,000 g for 10 minutes. The supernatant (250 μL) was collected and diluted 5 times for analysis. For preparation of the urine samples, enzymatic deconjugation of the samples was performed as described previously[16]. In brief, 50 μL from each group (control and treated) were treated with β-glucuronidase (250 U) and sulfatase (3 U) for 45 min at 37 °C and extracted twice with ethyl acetate. The ethyl acetate fraction was dried under vacuum, and the solid was resuspended in 1.25 mL of 80% aqueous methanol with 0.2% acetic acid for further analysis.

Separation of the M2 isomers using preparative HPLC

Waters (Milford, MA) preparative HPLC systems with 2545 binary gradient module, Waters 2767 sample manager, Waters 2487 autopurification flow cell, Waters fraction collector III, dual injector module, and 2489 UV/Visible detector were used to separate M2 isomers. A Phenomenex (Torrence, CA) Gemini-NX C_{18} column (250 mm × 30.0 mm i.d., 5 μm) was used with a flow rate of 20.0 mL/min. The wavelength of UV detector was set at 280 nm. The injection volume was 1.0 mL for each run. The mobile phase consisted of solvent A (H_2O + 0.1% formic acid) and solvent B (MeOH + 0.1% formic acid). M2 (5 mg/mL) was injected to the preparative column and eluted with a gradient solvent system (0% B from 0 to 5 min; 0 to 45% B from 5 to 15 min; 45 to 55% B from 15 to 25 min; 55 to 75% B from

25 to 45 min; then 0% B from 45 to 50 min). The fractions were analyzed and collected by an HPLC-ECD/UV system (ESA, Chelmsford, MA) consisting of an ESA model 584 HPLC pump, an ESA model 542 autosampler and an ESA organizer. The chromatographic analysis was performed on a chiral C_{18} column of Lux Amylose-2 (150 mm × 4.6 mm i.d., 5 μm, Phenomenex) at a flow rate of 1.0 mL/min. The mobile phase consisted of solvent A (20 mM NH_4OAc aqueous solution + 0.1% TFA) and solvent B (MeCN + 0.1% TFA). Isocratic elution (20% B in 30 min) was used to analyze M2. A total of 10 runs on prep-HPLC resulted in 8 mg of M2-1 (t_R 19.1 min) and 15 mg of M2-2 (t_R 20.6 min). Both M2-1 and M2-2 were white solids. ^1H, ^{13}C, and two- dimensional (2-D) NMR spectra of the two compounds were acquired on a Bucker AVANCE 600 MHz instrument (Brucker, Inc., Silberstreifen, Rheinstetten, Germany). M2-1 and M2-2 were analyzed in CD_3OD. ^1H and ^{13}C NMR data of M2-1 and M2-2 are listed in Table 1.

HPLC analysis

An HPLC-ECD (ESA, Chelmsford, MA) consisting of an ESA model 584 HPLC pump, an ESA model 542 autosampler, an ESA organizer, and an ESA electrochemical detector (ECD) coupled with two ESA model 6210 four sensor cells was used for analyzing the metabolic profiles of 6S and M2. A Gemini C_{18} column (150 mm × 4.6 mm, 5 μm; Phenomenex, Torrance, CA) was used for chromatographic analysis at a flow rate of 1.0 mL/min. The mobile phases consisted of solvent A (30 mM sodium phosphate buffer containing 1.75% acetonitrile and 0.125% tetrahydrofuran, pH 3.35) and solvent B (15 mM sodium phosphate buffer containing 58.5% acetonitrile and 12.5% tetrahydrofuran, pH 3.45). The gradient elution had the following profile: 20% B from 0 to 3 min; 20–55% B from 3 to 11 min; 55–60% B from 11 to 12 min; 60–65% B from 12 to 13 min; 65–100% B from 13 to 40 min; 100% B from 40 to 45 min; and then 20% B from 45.1 to 50 min. The cells were then cleaned at a potential of 1000 mV for 1 min. The injection volume of the sample was 10 μL. The eluent was monitored by the Coulochem electrode array system (CEAS) with potential settings at −100, 0, 100, 200, 300, 400, and 500 mV. Data for Figures 2 and 4 were from the channel set at 300 mV of the CEAS.

LC/APCI-MS method

LC/MS analysis was carried out with a Thermo-Finnigan Spectra System, which consisted of an Accela high-speed MS pump, an Accela refrigerated autosampler, and an LTQ Velos ion trap mass detector (Thermo Electron, San Jose, CA) incorporated with atmospheric-pressure chemical ionization (APCI) interfaces. A Gemini C_{18} column (150 × 4.6 mm i.d., 5 μm; Phenomenex, Torrance, CA) was used for separation at a flow rate of 0.7 mL/min. The column was eluted from 100% solvent A (5% aqueous methanol with 0.2% acetic acid) for 1 min, followed by linear increases in B (95% aqueous methanol with 0.2% acetic acid) to 55% from 1 min to 4 min, to 85% from 4 to 25 min, to 100% from 25 to 30 min, and then with 100% B from 30 to 35 min. The column was then re-equilibrated with 100% A for 5 min. The LC eluent was introduced into the APCI interface. The positive ion polarity mode was set for the APCI source with the voltage on the APCI interface maintained at approximately 4.5 kV. Nitrogen gas was used as the sheath gas and auxiliary gas. Optimized source parameters, including APCI capillary temperature (330 °C), vaporizer temperature (400 °C), sheath gas flow rate (45 units), auxiliary gas flow rate (20 units), and tube lens (50 V), were tuned using authentic M2. The collision-induced dissociation (CID) was conducted with an isolation width of 2 Da and normalized collision energy of 35 for MS^2 and MS^3. Default automated gain control target ion values were used for MS – MS^3 analyses. The mass range was measured from 100 to 1000 *m/z*. Data acquisition was performed with Xcalibur version 2.0 (Thermo Electron, San Jose, CA, USA).

Stability of M2

To test the stability of M2 in various chemical environments, compound was dissolved in DMSO (10 mM) and diluted with each respective test solution (H_2O, MeOH, PBS buffer (pH = 7.4) and McCoy's 5A medium) to 10 μM. These conditions were incubated at 37°C in 5% CO_2 incubator and samples were harvested at different time points over the course of 24 hours. The compound and degradation products were analyzed by HPLC-ECD.

Metabolism of 6S and M2 in cancer cells and modulation of metabolism by GSH

Cells (1.0×10^6) were plated in 6-well culture plates and allowed to attach for 24 h at 37°C in 5% CO_2 incubator. 6S or M2 (in DMSO) was added to McCoy's 5A medium (containing 10% fetal bovine serum, 1% penicillin/streptomycin, and 1% glutamine) to reach a final concentration of 10 μM, in the absence or presence of GSH (5 mM) and was incubated with cancer cell lines HCT-116 and H-1299. At different time points (0, 30 min, 1, 2, 4, 8, and 24 h), 190 μL samples of supernatant were taken and transferred to vials containing 10 μL of 0.2% ascorbic acid to stabilize 6S, M2, and their respective metabolites. An equal volume of acetonitrile was added to the samples before centrifugation. The supernatant was harvested and the samples were analyzed by HPLC-ECD.

Modulation of the growth inhibitory effects of 6S, M2 and M13 against human cancer cells by GSH

Cell growth inhibition was determined by a 3-(4,5-dimethylthiazol-2-yl)-2,5-diphenyltetrazolium bromide (MTT) colorimetric assay[22]. Human colon cancer (HCT-116) and human lung cancer (H-1299) cells (3000 cells/well) were plated in 96-well microtiter plates and allowed to attach for 24 h at 37 °C. The test compounds (in DMSO) were added to cell culture medium to desired final concentrations (0 – 120 μM; final DMSO concentrations for control and treatments were 0.1 %) in the absence and presence of 5 mM of GSH. After the cells were cultured for 24 h, the medium was aspirated and the cells were treated with 200 μL fresh medium containing 2.41 mmol/L MTT. After incubation for 3 h at 37 °C, the medium containing MTT was aspirated, 100 μL of DMSO was added to solubilize the formazan precipitate, and the plates were shaken gently for an hour at room temperature. Absorbance values were derived from the plate reading at 550 nm on a microtiter plate reader. The reading reflected the number of viable cells and was expressed as a percentage of viable cells in the control. Both HCT-116 and H-1299 cells were cultured in McCoy's 5A medium. All of the above media were supplemented with 10 % fetal bovine serum, 1 % penicillin/streptomycin, and 1 % glutamine, and the cells were kept in a 37 °C incubator with 95% humidity and 5% CO2.

Modulation of apoptosis induction of 6S, M2, and M13 in human cancer cells by GSH

Human colon cancer (HCT-116) and human lung cancer (H-1299) cells (3000 cells/well) were plated in 96-well microtiter plates and allowed to attach for 24 h at 37 °C. The test compounds (in DMSO) were added to cell culture medium to desired final concentrations (0 – 120 μM; final DMSO concentrations for control and treatments were 0.1 %), in the absence or presence of 5 mM GSH. After 24 hours, media containing compound was removed and cells were lysed in their respective wells with reagents from a Cell Death Detection ELISA^{PLUS} kit from Roche Applied Science (Mannheim, Germany). Samples were harvested after cell lysates were spun down at 300g for 10 minutes. To streptavidin coated microplates, 20μL samples were added, and mixed with 80μL Immunoreagent, which consisted of anti-histone-biotin, and anti-DNA-POD, and incubated with gentle shaking for 2 hours at room temperature. After incubation, Immunoreagent was removed and samples were washed 3 times with 250 μL incubation buffer. Substrate solution, ABTS, was added to each well and color was developed for 15 minutes before stopping the reaction with ABTS

stop solution and reading absorbance on a microplate reader at 430nm. Experiments were performed in triplicate and the average is given in comparison to DMSO control with standard deviation.

Statistical analysis

For simple comparisons between two groups, two-tailed Student's *t*-test was used. A p-value of less than 0.05 was considered statistically significant in all the tests.

Results

Stability of M2

We have reported that cysteine-conjugated metabolite of 6S, M2, has comparable bioactivity to 6S in cancer cells but has much less toxicity than 6S in normal cells[18]. M2 is the Michael addition product of 6S, which led us to suspect that there is a state of equilibrium between the parent compound and its conjugated metabolite. We then investigated the stability of M2 in H_2O, MeOH, PBS buffer (pH = 7.4) and McCoy's 5A medium (Figure S1, Supporting Information). Our results showed M2 was stable in H_2O and MeOH up to 24 hours, while it was quickly decomposed in PBS buffer (pH = 7.4) and McCoy's 5A medium to form 6S. Most of M2 was de-conjugated to form 6S in 3 hours. Our results clearly indicate that the stability of M2 is pH dependent. The compound was stable in acidic and neutral conditions but quickly decomposed in slightly basic solution, such as a physiological condition with pH of 7.4. Metabolites 5-N-acetylcysteinyl-[6]-shogaol (M5) and 5-glutathionyl-[6]-shogaol (M13), which are also Michael addition products[18], had higher stability than M2 in the four conditions above. Among these three metabolites, M13 was more stable than M2, with M5 as the most stable metabolite in physiological conditions (pH = 7.4) (data not shown). Based on our previous report on the bioactivity of these three metabolites, we know the stability of the compounds is important to their subsequent efficacy, which led us to suspect that these metabolites act as putative carriers of 6S.

Metabolism of M2 in cancer cells with or without GSH

To test our hypothesis, we then investigated the metabolism of M2 in different cells. After incubation of M2 with two cancer cell lines (HCT-116, and H-1299), the culture media were collected at different time points and analyzed by HPLC-ECD. Our results indicate that M2 was extensively metabolized in both cancer cell lines (Figure 2A and 2B). M2 was decomposed to 6S in the first 2 hours in both cell lines, which was supported by the apparent increase of 6S abundance (Figure 2A and 2B). After 24 h incubation, four major metabolites appeared in HCT-116 human colon cancer cells. They were identified as M6, M9, M11, and M13 by comparing their retention times and tandem mass fragments with those of our purified authentic standards (data not shown). Both M9 and M11 were detected as the major metabolites of M2 in H-1299 human lung cancer cells (Figure 2B). At 24 h, M2 was almost completely converted to M9 and M11 in H-1299 cells. Our results clearly show that M2 has a similar metabolic profile to the previously reported profile of 6S[16]. Investigation of M13 metabolism also indicated a similar pathway to that of 6S (data not shown). In general, the thiol-conjugates in aqueous solution exist in equilibrium with their free forms, which possess electrophilic reactivity. Consequentially, an excess of exogenous GSH can significantly affect the equilibrium. To examine the effect of excess GSH on the metabolism of M2 and 6S, HCT-116 and H-1299 cells were simultaneously treated with a physiological concentration of GSH (5 mM) and M2 (10 μM) or 6S (10 μM). As shown in Figure 2C–2F, GSH excess decelerated the metabolism of both M2 and 6S to their corresponding metabolites. At 24 hrs, the abundance of all redox metabolites was dramatically less than the amounts in GSH untreated samples. Our results show 6S in the culture media was

presumably conjugated with the excess moles of GSH, thus blocking intracellular uptake of 6S.

GSH affects the bioactivity of 6S, M2, and M13

Cell death was analyzed by an MTT colorimetric assay, as described in the experimental section. In the presence of excess GSH, the IC_{50} values of 6S, M2, and M13 against HCT-116 cells increased to 109.4, 112.0, and greater than 120 μM from 20.6, 36.8, and 43.6 μM, respectively, indicating compound potency was greatly diminished (Figure 3A). A similar effect was seen in H-1299 cells, in which addition of excess GSH caused IC_{50} values to increase to more than 120 μM for 6S, M2, and M13, versus 20.7, 25.7, and 45.18 μM, respectively (Figure 3B).

Apoptosis is a major mechanism of regulation allowing cells to undergo cell death upon activation of specific external and/or internal pathways. Hence, we investigated the role of GSH on the induction of apoptosis by active compounds 6S, M2, and M13, in human cancer cells. As shown in Figure 3C and 3D, treatment of excess GSH in conjunction with test compounds diminished apoptotic induction significantly. In HCT-116 cells, 6S apoptosis induction after 20 μM treatment was reduced from almost 6-fold (no GSH) to just over 2-fold (with GSH). Similarly, induction of apoptosis in H-1299 cells after 20 μM M2 treatment was reduced from almost 4-fold (no GSH) to slightly over baseline (with GSH). Activation of apoptosis by 40 μM M13 was also reduced by excess GSH from 3-fold to 2-fold induction, compared to DMSO control.

Metabolism of M2 in mice

Since both 6S and M2 showed similar metabolic profiles *in vitro*, we investigated the metabolism of 6S and M2 in mice to compare their *in vivo* biotransformations. In this study, we used HPLC/ECD and LC/APCI/MS to analyze the metabolic profiles of 6S and M2 in our samples. Representative HPLC chromatograms of the metabolites detected in mouse fecal and urinary samples collected after the administration of 200 mg/kg of 6S or M2 through oral gavage are shown in Figure 4. Similar metabolic profiles for both 6S and M2 were derived from urine samples (Figure 4A and 4B), which was further confirmed by LC/MS (Figure 4E and 4F). The fecal samples collected from 6S or M2 treated mice also showed similar metabolic profiles with the exception of differences in abundances of M5 and its 3′-demethylated product (M16). This indicated that in addition to acting as a carrier of 6S, M2 is also directly acetylated to M5, which is further demethylated to M16 *in vivo*. All thiol-conjugated metabolites, M1–M5, M10, and M12 were identified by comparing their retention times and mass spectra with those of authentic standards. Metabolites M16–M21 were identified by analysis of their tandem mass spectra.

Identification of metabolites M16-M21

In the extracted ion chromatogram of m/z 426 $[M + H]^+$, two peaks (M16, RT: 18.65, and 18.88 min, respectively) were observed from fecal samples collected from 6S and M2 treated mice (Figure 5A). These two peaks had the molecular weight of 425, which was further confirmed by the observation of mass ions at m/z 448 $[M + Na]^+$, and 851 $[2M + H]^+$ (spectra were not shown). The molecular weight of M16 is 14 Da less than that of 5-N-acetylcysteinyl-6S (M5, M.W.: 439) indicating they are feasibly demethylated M5. In order to corroborate this proposition, we compared the tandem mass spectra of m/z 426 of these two peaks with the tandem mass spectra of M5. Our results indicated M16's major product ion was m/z 263 (MS^2: m/z 426), while M5 showed its major product ion with m/z 277 (MS^2: m/z 440), which is 14 Da higher than that of M16. In addition, the MS^3 spectrum of the product ion m/z 263 (MS^3: m/z 263/426) of M16 showed its major product ion with m/z 123, which is 14 Da less than that of the MS^3 spectrum of the product ion m/z 277 (MS^3: m/

z 277/440) of M5. All of the above evidence suggests that M16 is the demethylated product of M5. A detailed potential fragmentation pathway of M16 is shown in Figure 5D. Since there is only one methyl group in M5, M16 was thus identified as 3′-demethylated M5. Due to the presence of one chiral center (C-5) in M16, we suspect that the two peaks are diastereomers of M16.

In the extracted ion chromatogram of m/z 341 $[M + H]^+$ (monooxygenation of M10 under positive mode), two new peaks (M17, RT: 14.61, and 15.28 min, respectively) were observed from urine and fecal samples collected from 6S and M2 treated mice (Figure 5B). It is reported that many xenobiotics featuring a thioether group are easily metabolized into sulfoxides and sulfones in reactions catalyzed by flavin-containing monoxygenases and/or cytochrome P450[23, 24]. Since 5-methylthio-1-(4′-hydroxy-3′-methoxyphenyl)-decan-3-one (M10) has been reported as a major metabolite of 6S, we then predicted these two peaks as potential sulfoxide metabolites of M10. Essentially, M17 showed its major product ion at m/z 277 (loss of a HSOMe, molecular ion of 6S under positive mode). In addition, the MS^3 mass spectra of this product ion (MS^3: m/z 277/341) showed the same tandem mass as that of 6S (MS^2: m/z 277)[18], which further confirmed our deduction. A detailed potential fragmentation pathway of M17 is shown in Figure 5D. Due to the presence of one chiral center (C-5) in M17, we tentatively identified the two peaks as diastereomers of M17.

Two peaks (M18, RT: 12.51, and 13.19 min, respectively) were observed in the extracted chromatogram of m/z 327 $[M + H]^+$ in the urine and fecal samples collected from 6S and M2 treated mice (Figure 5C). These two peaks showed 14 Da less than that of M17, indicating they were potential mono-demethylated M17. This was further confirmed by observing m/z 263 $[M + H]^+$ (loss of one CH_3SOH moiety from M18) as one of the major product ions in the MS^2 spectrum of molecular ion m/z 327 $[M + H]^+$ (Figure 5C). The MS^3 spectrum (MS^3: m/z 263/327) of m/z 263 showed m/z 123 as the major product ion, which is a typical product ion for the demethylated compounds (Figure 5D). Since there was only one methyl group in M17, we identified M18 as 3′-demethylated M17. Similar to our analysis of M17, we tentatively identified the two peaks as diastereomers of M18.

In our previous study, ketone (C-3) reduced metabolites of 6S and its thiol conjugates were detected in 6S treated mice as the major biotransformation products. Similarly, corresponding ketone reduced metabolites of M16–M18 were detected in mouse urine and fecal samples after treatment with 6S or M2, and were named M19–M21, respectively (Structure elucidation of M19-M21 is shown in Supporting Information).

Isolation, identification, and bioactivity of M2 diastereoisomers

M2 was synthesized from 6S in our laboratory[18]. Stereochemistry frequently affects the biological activity and pharmacokinetic profile of a drug. Hence, it is a challenging yet necessary endeavor to separate synthetic stereoisomers. Previously we reported the separation of the diastereomers of M13 (GSH conjugates of 6S) using a non-chiral preparative HPLC column. Here, separation of M2 isomers on preparative HPLC in conjunction with fraction collection guided by chiral analytic HPLC (see Experimental Section) led to two diastereoisomers, M2-1 and M2-2, which displayed almost duplicate ^1H and ^{13}C NMR spectra (Table 1). The major differences were the ^1H signals for H-5 (δ_H 3.12 in M2-1 vs. 3.09 in M2-2) and the ^{13}C signals for C-5 (δ_C 42.3 in M2-1 vs. 41.3 in M2-2) (Figure 6). Their NOESY spectra showed the correlations between H-1″b (δ_H 2.84) and H-5 (δ_H 3.12) in M2-1 and H-1″a (δ_H 3.17) and H-5 (δ_H 3.09) in M2-2, indicating that H-5 in M2-1 had the same orientation as that of H-1″b while H-5 in M2-2 had the same configuration as that of H-1″a (Figure 6). It is well known that H-2″ in a L-cysteinyl residue has the *R* absolute configuration (Figure 6). The coupling constant (J = 9.3 Hz) of H-1″b (δ_H 2.84) with H-2″ (δ_H 3.63) in M2-1 and that (J = 3.7 Hz) of H-1″a (δ_H 3.17) with H-2″ (δ_H

3.62) in M2-2 suggested that H-1″a has the same *R* configuration as that of H-2″ while H-1″b has the *S* configuration. Therefore, the absolute configurations of H-5 in M2-1 and M2-2 were tentatively assigned as *S* and *R*, respectively (Figure 6).

In order to investigate the influence of stereochemistry on activity, cancer cells HCT-116 and H-1299 were treated with M2 or its constituent stereoisomers (M2-1 and M2-2) individually, with concentrations ranging from 0 to 80 μM. M2-2 exhibited a similar activity to M2, and a slightly higher potency than its stereoisomer M2-1 in both HCT-116 and H-1299 cells, with IC_{50} values of 25.5 μM and 20.63 μM versus 40.44 μM and 36.43 μM, for each isomer, respectively (Figure 6C and 6D).

Discussion

Previous studies in our group have shown that cysteine-conjugated metabolites of 6S possess chemopreventative activity comparable to the parent compound[18]. The means by which the thiol-conjugates of electrophiles, such as M2 (5-cysteinyl-[6]-shogaol), yield their bioactivities have been studied to some extent. There is speculation as to whether the conjugates themselves have unique potency or act as carriers of their parent molecules and deconjugate before exerting their effects. Our work in this study supported the latter notion, beginning with a series of tests of the chemical stabilities of M2 in various solutions, which showed a favored decomposition of conjugates to free 6S at physiological pH (7.4). Further, we found that in the presence of excess GSH, deconjugation of the putative carriers was delayed, as noted by their postponed metabolic transformations via initial degradation to free 6S, which was able to enter the cell, and followed by the expected reductive metabolism of 6S. The reduced bioactivities of 6S and thiol-conjugates M2 and M13 in the presence of excess GSH also supported the notion of these compounds as carriers. Bioactivity of 6S was likely reduced by the abundance of thiol groups available for Michael addition, thus delaying entry into the cell by conjugation. Similarly, M2 and M13 deconjugation was likely deferred due to thermodynamic equilibrium favor, thus delaying free 6S cell entry (Figure 7). Evidence for the latter is presented thoroughly for ITC's in a study in which cytochrome P450 enzymes known to metabolically activate pre-carcinogens were subjected to both ITCs and their cysteine conjugates. It was found that decomposition of conjugates occurred favorably at physiological pH and the rate of de-conjugation determined their potencies as P450 inhibitors indicating these conjugates as carriers of the free ITCs[19]. A similar study of ITCs proposed that thiols may not act as antioxidants in ITCs studies, but rather block intracellular uptake, thereby showing reduced electrophilic activity of these compounds[26].

Thiol-conjugated metabolites of other highly electrophilic compounds have been studied, such as sulforaphane (SFN) and its N-acetylcysteine conjugate (SFN-NAC). Sulforaphane is a phytochemical abundant in cruciferous vegetables such as broccoli or cabbage, which have been associated with chemoprevention[27]. Its primary excretion product *in vivo* is SFN-NAC, which has been shown to retain the anti-cancer activity of its parent SFN. For example, lung adenoma formation was induced in A/J mice by tobacco pre-carinogen NNK, and significant and comparable reductions in adenocarincoma multiplicity were noted in mice fed 1.5 μmol/g diet sulforaphane (multiplicity reduction of 70%), as well as mice fed 4 μmol/g diet sulforaphane-*N*-acetylcysteine (multiplicity reduction also 70%)[28]. SFN and SFN-NAC were also found to have similar activities against human prostate cancer cells, in which apoptosis was induced by 30 h exposure to 50 μM SFN (52% apoptotic cells) or SFN-NAC (40% apoptotic cells)[29]. These data are somewhat consistent with our findings that cysteine-conjugated metabolite M2 retains similar bioactivity to its parent 6S.

After establishing M2 as a likely carrier of 6S *in vitro*, M2 metabolism was observed *in vivo*. As a carrier of 6S, M2 was expected to yield a metabolic profile similar to that of its

parent molecule. While there are differences in the abundances of two major metabolites (M5 and M16) in fecal samples of M2 treated mice, the similarities of the profiles indicate that M2 is also transformed *in vivo* to 6S, to yield the observed likenesses between their metabolic routes. Thus, metabolically, M2 appears to act primarily as a carrier of 6S in addition to acting as an independent compound. M2, as an intermediate of the mercapturic acid pathway, can be directly metabolized to form M5, which can be further transformed to its demethylated metabolite (M16). In the current study, we did not find M16 in urine samples from mice treated with 6S or M2, but rather in the fecal samples, which suggested demethylation was probably conducted by microbiota in the colon. This is a valid topic for future work, as well as whether the resultant metabolites identified in this study display novel bioactivity. Previously we reported the separation of diastereomers of M13 and tested bioactivity of the two isomers. We found M13 as the mixture of M13-1 and M13-2 had slightly better growth inhibitory effects on cancer cells than the two diastereomers alone, and that M13-1 and M13-2 had similar activity, though M13-2 was slightly more potent than M13-1. Here, we separated the two diastereomers of M2, M2-1 and M2-2, and tested their bioactivities in HCT-116 human colon cancer cells and H-1299 human lung cancer cells. Our results indicated M2 as the mixture of M2-1 and M2-2 had similar growth inhibitory effects on cancer cells as that of M2-2, and had better growth inhibitory effects than M2-1 on cancer cells. More importantly, we did observe M2 as the metabolite of 6S in the form of a mixture of M2-1 and M2-2 in mice (Figure S3, Supporting Information). The ratio of the two isomers in mouse urine and feces is slightly different from the ratio in synthetic M2.

The impetus of this study was to elucidate the mechanism by which cysteine-conjugated metabolite of 6S, M2, exerts its bioactivity. The methods employed were guided by the premise that M2 acts as a carrier of 6S, and is likely degraded before exerting activity. Our results indicate that this proposed mechanism is likely, and that further study of the bioactivities of 6S thiol-conjugates is warranted.

Supplementary Material

Refer to Web version on PubMed Central for supplementary material.

Acknowledgments

Funding Support: Funding for this investigation was provided by grants CA138277 (S. Sang) from the National Cancer Institute and CA138277S1 (S. Sang) from National Cancer Institute and Office of Dietary Supplement of National Institutes of Health.

Abbreviations

6S	[6]-shogaol
APCI	atmospheric-pressure chemical ionization
GSH	glutathione
HPLC	high-performance liquid chromatography
LC/MS	liquid chromatrography/mass spectrometry
M2	5-cysteinyl-[6]-shogaol
M5	5-N-acetylcysteinyl-[6]-shogaol
M13	5-glutathionyl-[6]-shogaol

References

(1). Langner E, Greifenberg S, Gruenwald J. Ginger: history and use. Adv Ther. 1998; 15:25–44. [PubMed: 10178636]

(2). Altman RD, Marcussen KC. Effects of a ginger extract on knee pain in patients with osteoarthritis. Arthritis Rheum. 2001; 44:2531–2538. [PubMed: 11710709]

(3). Ali BH, Blunden G, Tanira MO, Nemmar A. Some phytochemical, pharmacological and toxicological properties of ginger (Zingiber officinale Roscoe): a review of recent research. Food Chem Toxicol. 2008; 46:409–420. [PubMed: 17950516]

(4). Kubra IR, Rao LJ. An impression on current developments in the technology, chemistry, and biological activities of ginger (Zingiber officinale Roscoe). Crit Rev Food Sci Nutr. 2012; 52:651–688. [PubMed: 22591340]

(5). Kundu JK, Na HK, Surh YJ. Ginger-derived phenolic substances with cancer preventive and therapeutic potential. Forum Nutr. 2009; 61:182–192. [PubMed: 19367122]

(6). Shukla Y, Singh M. Cancer preventive properties of ginger: a brief review. Food Chem Toxicol. 2007; 45:683–690. [PubMed: 17175086]

(7). Surh YJ, Lee E, Lee JM. Chemoprotective properties of some pungent ingredients present in red pepper and ginger. Mutat Res. 1998; 402:259–267. [PubMed: 9675305]

(8). Surh YJ, Park KK, Chun KS, Lee LJ, et al. Anti-tumor-promoting activities of selected pungent phenolic substances present in ginger. J Environ Pathol Toxicol Oncol. 1999; 18:131–139. [PubMed: 15281225]

(9). Park EJ, Pezzuto JM. Botanicals in cancer chemoprevention. Cancer Metastasis Rev. 2002; 21:231–255. [PubMed: 12549763]

(10). Aggarwal BB, Shishodia S. Molecular targets of dietary agents for prevention and therapy of cancer. Biochem Pharmacol. 2006; 71:1397–1421. [PubMed: 16563357]

(11). Kim JS, Lee SI, Park HW, Yang JH, et al. Cytotoxic components from the dried rhizomes of Zingiber officinale Roscoe. Arch Pharm Res. 2008; 31:415–418. [PubMed: 18449496]

(12). Bak MJ, Ok S, Jun M, Jeong WS. 6-shogaol-rich extract from ginger upregulates the antioxidant defense systems in cells and mice. Molecules. 2012; 17:8037–8055. [PubMed: 22763741]

(13). Hu R, Zhou P, Peng YB, Xu X, et al. 6-Shogaol induces apoptosis in human hepatocellular carcinoma cells and exhibits anti-tumor activity in vivo through endoplasmic reticulum stress. PLoS One. 2012; 7:e39664. [PubMed: 22768104]

(14). Sang S, Hong J, Wu H, Liu J, et al. Increased growth inhibitory effects on human cancer cells and anti-inflammatory potency of shogaols from Zingiber officinale relative to gingerols. J Agric Food Chem. 2009; 57:10645–10650. [PubMed: 19877681]

(15). Wu H, Hsieh MC, Lo CY, Liu CB, et al. 6-Shogaol is more effective than 6-gingerol and curcumin in inhibiting 12-O-tetradecanoylphorbol 13-acetate-induced tumor promotion in mice. Mol Nutr Food Res. 2010; 54:1296–1306. [PubMed: 20336681]

(16). Chen H, Lv L, Soroka D, Warin RF, et al. Metabolism of [6]-shogaol in mice and in cancer cells. Drug Metab Dispos. 2012; 40:742–753. [PubMed: 22246389]

(17). Chen H, Sang S. Identification of phase II metabolites of thiol-conjugated [6]-shogaol in mouse urine using high-performance liquid chromatography tandem mass spectrometry. J Chromatogr B Analyt Technol Biomed Life Sci. 2012; 907:126–139.

(18). Zhu Y, Warin RF, Soroka DN, Chen H, et al. Metabolites of ginger component [6]-shogaol remain bioactive in cancer cells and have low toxicity in normal cells: chemical synthesis and biological evaluation. PLoS One. 2013; 8:e54677. [PubMed: 23382939]

(19). Conaway CC, Krzeminski J, Amin S, Chung FL. Decomposition rates of isothiocyanate conjugates determine their activity as inhibitors of cytochrome p450 enzymes. Chem Res Toxicol. 2001; 14:1170–1176. [PubMed: 11559030]

(20). Zhang Y. The molecular basis that unifies the metabolism, cellular uptake and chemopreventive activities of dietary isothiocyanates. Carcinogenesis. 2011; 33:2–9. [PubMed: 22080571]

(21). Conaway CC, Krzeminski J, Amin S, Chung FL. Decomposition rates of isothiocyanate conjugates determine their activity as inhibitors of cytochrome p450 enzymes. Chemical Research in Toxicology. 2001; 14:1170–1176. [PubMed: 11559030]

(22). Mosmann T. Rapid colorimetric assay for cellular growth and survival: application to proliferation and cytotoxicity assays. J Immunol Methods. 1983; 65:55–63. [PubMed: 6606682]

(23). Mitchell SC, Waring RH. The early history of xenobiotic sulfoxidation. Drug Metabolism Reviews. 1985; 16:255–284. [PubMed: 3914937]

(24). Usmani KA, Karoly ED, Hodgson E, Rose RL. In vitro sulfoxidation of thioether compounds by human cytochrome P450 and flavin-containing monooxygenase isoforms with particular reference to the CYP2C subfamily. Drug Metab Dispos. 2004; 32:333–339. [PubMed: 14977868]

(25). Chen H, Soroka DN, Hu Y, Chen X, et al. Characterization of thiol-conjugated metabolites of ginger components shogaols in mouse and human urine and modulation of the glutathione levels in cancer cells by [6]-shogaol. Mol Nutr Food Res. 2013

(26). Mi L, Sirajuddin P, Gan N, Wang X. A cautionary note on using N-acetylcysteine as an antagonist to assess isothiocyanate-induced reactive oxygen species-mediated apoptosis. Anal Biochem. 2010; 405:269–271. [PubMed: 20541518]

(27). Murillo G, Mehta RG. Cruciferous Vegetables and Cancer Prevention. Nutrition and Cancer. 2001; 41:17–28. [PubMed: 12094621]

(28). Conaway CC, Wang CX, Pittman B, Yang YM, et al. Phenethyl isothiocyanate and sulforaphane and their N-acetylcysteine conjugates inhibit malignant progression of lung adenomas induced by tobacco carcinogens in A/J mice. Cancer Res. 2005; 65:8548–8557. [PubMed: 16166336]

(29). Chiao JW, Chung FL, Kancherla R, Ahmed T, et al. Sulforaphane and its metabolite mediate growth arrest and apoptosis in human prostate cancer cells. Int J Oncol. 2002; 20:631–636. [PubMed: 11836580]

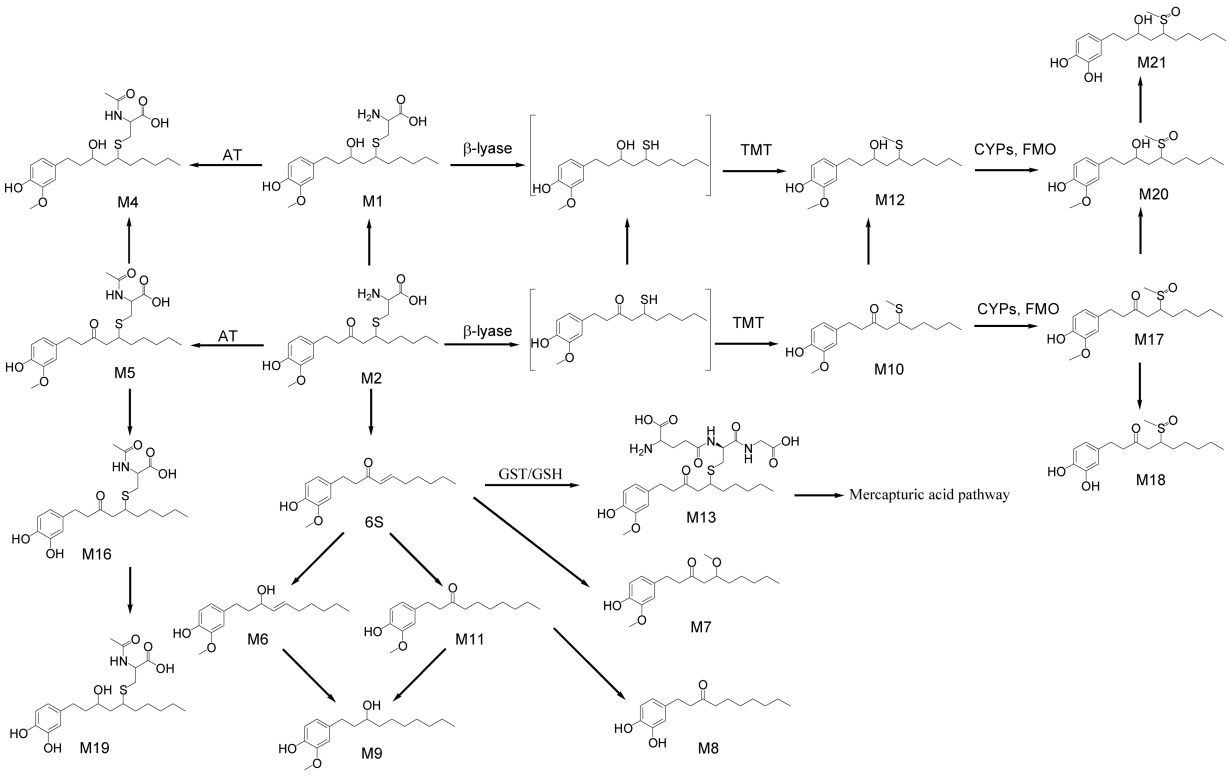

Figure 1.

Structures of cysteine-conjugated [6]-shogaol (M2) and its metabolites and potential biotransformation pathways of M2. AT: N-acetyltransferase; TMT: thiol methyltransferase; CYPs: cytochrome P450 enzymes; FMO: flavin monooxygenase.

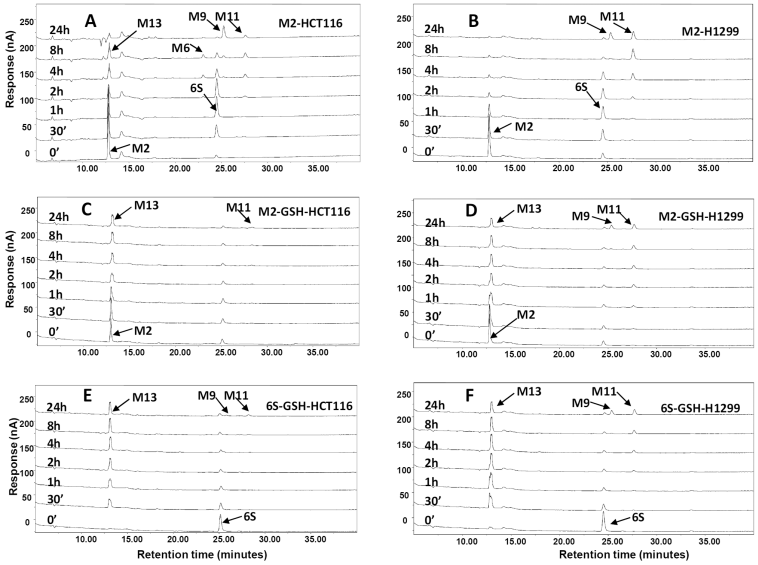

Figure 2.

HPLC-ECD traces of incubation mixtures from HCT-116 (A) and H-1299 (B) cell lines and impact of glutathione (5 mM) on the metabolism of M2 and [6]-shogaol (6S) in HCT-116 (C and E) and H-1299 (D and F) cell lines.

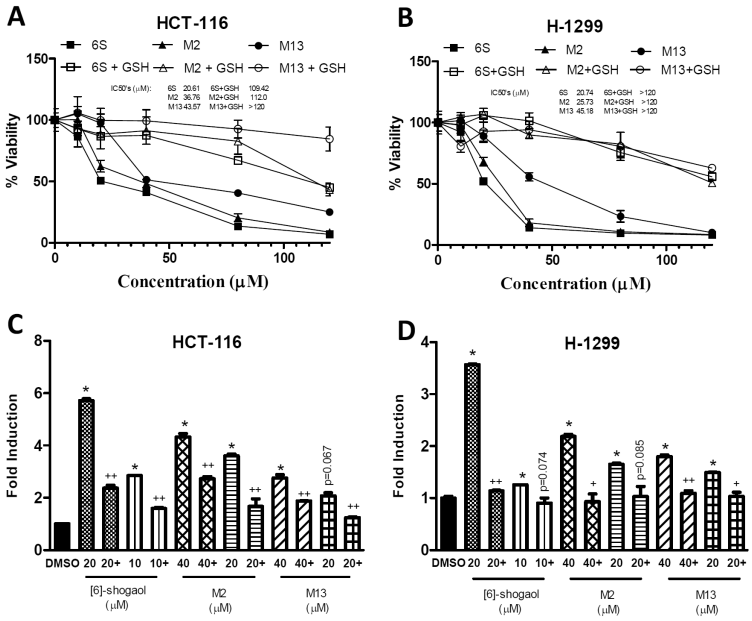

Figure 3.

Impact of glutathione (5 mM) on growth inhibitory effects (A and B) and apoptosis induction effects (C and D) of [6]-shogaol (6S), M2, or M13 against human colon cancer cells HCT-116 (A and C) and human lung cancer cells H-1299 (B and D). Cells were incubated with test compounds 6S, M2, or M13 with or without 5 mM GSH for 24 hours and were tested for cell viability or induction of apoptosis. (For growth inhibition assay, values are given as a percentage of positive control, n = 6. Bar, standard deviation. For induction of apoptosis, $*p < 0.05$,$**p < 0.01$, indicating significance of induction of apoptosis versus DMSO control. For impact of glutathione on induction of apoptosis, $^{+}p < 0.05$, $^{++}p < 0.01$, indicating significance of GSH inhibition of apoptosis.)

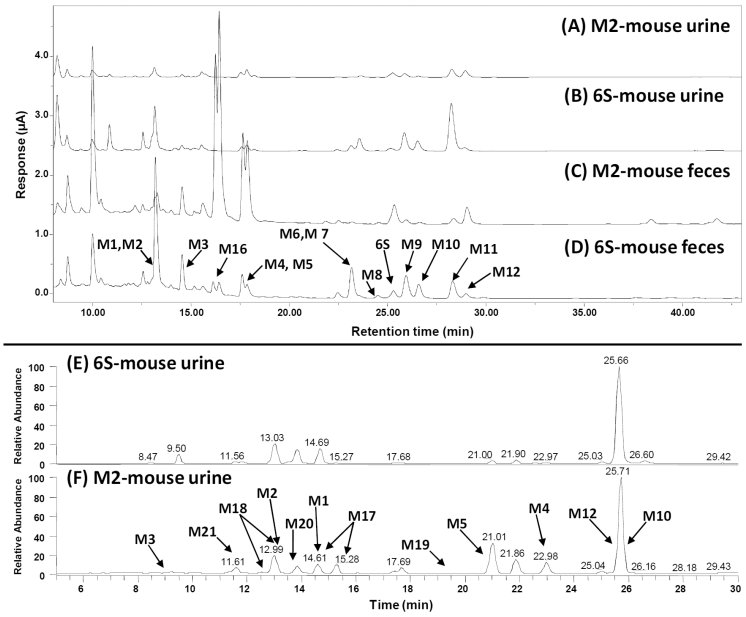

Figure 4.

Representative HPLC-ECD chromatograms of urine (A and B) and fecal (C and D) samples from mice treated with 200 mg/kg M2 (A and C) and [6]-shogaol (6S) (B and D); and extracted ion chromatograms of urine samples collected from [6]-shogaol (E) and M2 (F) treated mice obtained by positive APCI-MS interface.

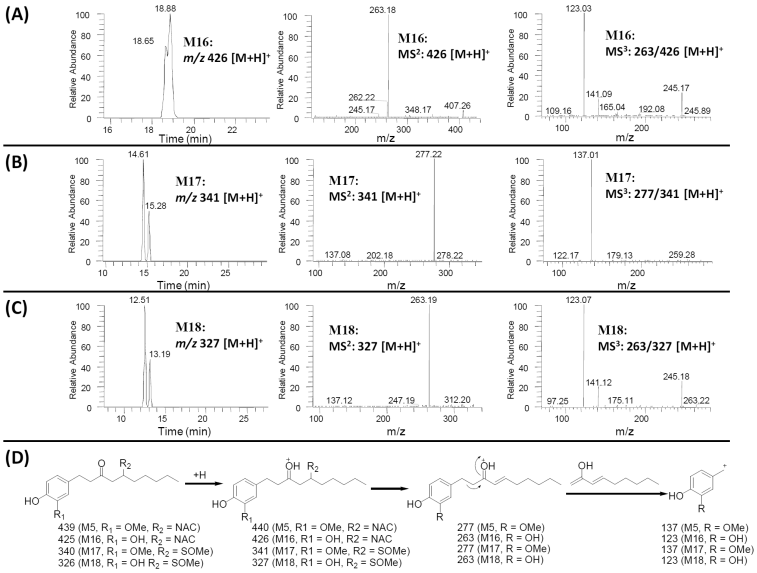

Figure 5.
LC-MS^2 and MS^3 (positive) spectra of M16 (A), M17 (B), and M18 (C), and a potential fragmentation pathway of M16–M18 (D).

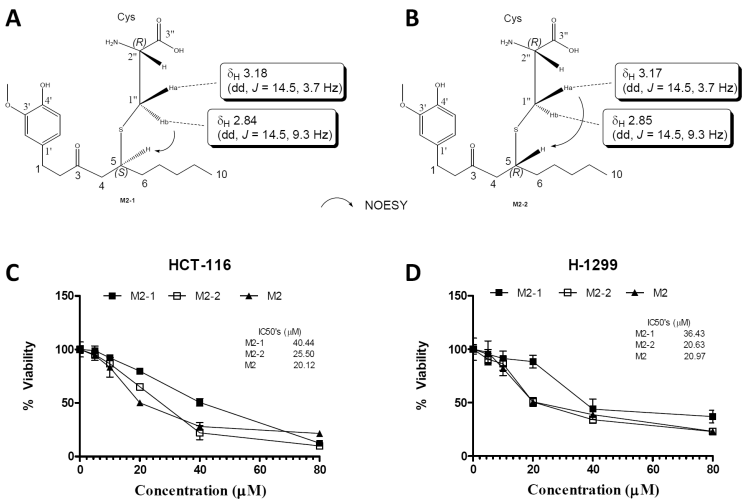

Figure 6.

Key NOESY correlations in M2-1 (A), M2-2 (B); and the major differences of the ^{1}H and ^{13}C NMR data of M2-1 (A) and M2-2 (B), respectively; growth inhibitory effects of M2, and its stereoisomers (M2-1 and M2-2) against human colon cancer cells HCT-116 (C) and human lung cancer cells H-1299 (D). Bar, standard error (n=6).

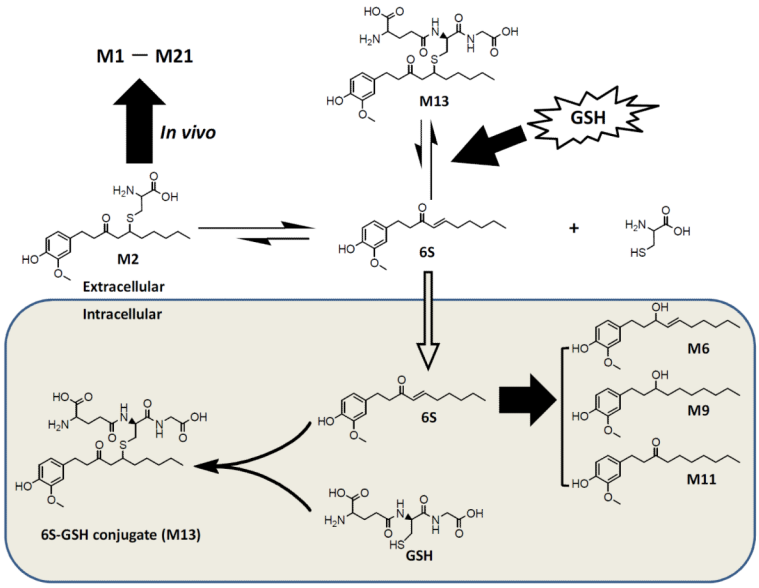

Figure 7.
Proposed mechanism for M2 serving as a carrier of [6]-shogaol *in vitro* and *in vivo*.

Table 1

δ_H (600 MHz) and δ_C (150 MHz) NMR spectra data of M2 isomers (M2-1 and M2-2) (CD_3OD, δ in ppm and *J* in Hz).

	M2-1		M2-2	
	δ_H multi (J)	**δ_C**	**δ_H multi (J)**	**δ_C**
1	2.77 m	30.3	2.77 m	30.3
2	2.74 m	45.7	2.74 m	45.9
3		211.7		211.8
4	2.71 m	49.6	2.71 m	49.6
	2.63 m		2.63 m	
5	3.12 m	42.3	3.09 m	41.3
6	1.53 m	36.3	1.53 m	36.8
7	1.39 m	27.5	1.39 m	27.4
8	1.28 m	32.6	1.28 m	32.6
9	1.33 m	23.6	1.33 m	23.6
10	0.891 (7.1)	14.4	0.89 t (7.0)	144.4
1′		133.9		133.8
2′	6.77 s	113.2	6.76 s	113.2
3′		148.9		148.9
4′		145.8		145.8
5′	6.67 d (8.0)	116.2	6.68 d (8.0)	116.2
6′	6.61 d (8.0)	121.8	6.62 d (8.0)	121.7
1″	a: 3.18 dd (14.5, 3.7)	32.8	a: 3.17 dd (14.5, 3.7)	32.8
	b: 2.84 dd (14.5, 9.3)		b: 2.85 dd (14.5, 9.3)	
2″	3.63 m	56.3	3.62 m	56.3
3″		172.6		172.6
*O*Me	3.82 s	56.4	3.82 s	56.4